Modeling of Stress−Strain Relations of Non-Gaussian Chains in Swollen Networks

Peter Cifra* and Tomáš Bleha

Polymer Institute, Slovak Academy of Sciences, 842 36 Bratislava, Slovak Republic

Received January 22, 1997; Revised Manuscript Received September 3, 1997

ABSTRACT: The results of the Monte Carlo (MC) simulations on a tetrahedral lattice are reported about the elastic response of model chains with variable segmental interaction and flexibility. The single-chain elastic functions were calculated either through distribution function $W(R)$ of end-to-end distances or the displacement R was directly computed for a given value of external force F. The computed force−displacement curves are strikingly affected by the chain-end constraints chosen, either of the "spring deformation" or of the "coil deformation" type, which correspond to the different physical situations. In all cases the elastic response is nonlinear and influenced by the solvent quality. The distribution function $W_F(R)$ of a chain prestretched by external force F and the corresponding relations f_F vs R were evaluated. By using the "three-chain model" of polymer networks the stress−strain isotherms were computed, which are directly relevant to the mechanical properties of the so-called c^* gels. The isotherms show non-Gaussian behavior with an upturn in stress at higher elongation modulated by the solvent quality. The consequences of the solvent-sensitive elastic functions of a network to the separability of the mixing and elastic terms in the Helmholtz energy of swelling are pointed out.

Introduction

The force−length relations for single flexible macromolecules are essential for rationalization of mechanical properties of polymer materials in solution and melt. The primary importance of these relations lies mainly in the subject of the rubber-like elasticity of amorphous cross-linked networks of flexible chains. The basic construction elements of such a network are molecular chains extending between cross-links of the network. In a traditional approach, the elastic response of the isolated network strands is determined at first and, subsequently, the properties of a network formed from strands are investigated.

Force (f)−length (R) relations for single linear macromolecules with end-to-end distance R can be calculated by several procedures,[1−5] particularly, (a) from the density distribution function of the end-to-end chain distance $W(R)$ or (b) by the computer simulations of a "deformation experiment" involving the stretching of a chain by an external force. This can be achieved[5] either by imposing the external tensile force on the chain ends and "measuring" the resulting deformed end-to-end distance R in the force direction ("stress ensemble") or by the increase of the end-to-end distance and measurement of the corresponding equilibrium force ("strain ensemble").

The first, traditional, method (a) makes use the probability density distribution function of the chain vector $W(\mathbf{R})$, or its spherically symmetrical part, the end-to-end distance distribution $W(R)$, which represents the distribution of molecules with one end fixed at the origin and the other end fixed in space by coordinates x, y, z. The density distribution functions $W(R)$ can be converted by a standard approach[1−3] into the related Helmholtz elastic energy difference ΔA_{el}:

$$\Delta A_{el} = A_R - A_f = -kT \ln W(R) \qquad (1)$$

where A_f is the mean configurational Helmholtz energy of a free chain and A_R is the related quantity for a chain with both ends fixed at the distance R. For the freely jointed chains the distribution function $W(R)$ can be approximated by a Gaussian function

$$W(R) = [3/(2\pi\langle R^2\rangle)]^{3/2} \exp[-3R^2/(2\langle R^2\rangle)] \qquad (2)$$

where $\langle R^2\rangle$ is the mean-square distance between the chain ends. The maximum of the function lies at $R = 0$, i.e., when the two ends of the chain are coincident.

The interrelation between ΔA_{el} and $W(R)$ is essential for the development of the theory of rubber elasticity since the tensile force f is determined by differentiation $f = d\Delta A_{el}/dR$. By definition, the direction of the force f is collinear with the chain vector $\mathbf{R}$. In the "ideal" case of the Gaussian chains, the force f is proportional to R, similarly to a Hookean spring (of zero unstrained length). The retractive character of the force favoring the return into the original state at $R = 0$ originates in this case solely from the entropy factors.

The analytical force−extension relations are available[1−4] for more complex freely jointed chain models that take into account the finite extensibility of the chains and predict nonlinear $f-R$ relations for single-chains that approach the Gaussian result at small elongations. In statistical treatments of real chains, the excluded volume (EV) effect is incorporated and contributes to a non-Gaussian character of the distribution function $W(R)$. Analytical functions representing $W(R)$ with EV display[5−7] a maximum located at small, finite values of R. By approaching $R = 0$, these functions $W(R)$ abruptly drop to zero ("correlation hole") since the chain ends with inherent volume cannot coincide. The force f derived from non-Gaussian distribution functions $W(R)$ with EV shows[5] a nonlinear dependence on R. The non-Gaussian distribution functions $W(R)$ were frequently employed[8−11] in the theory of rubber elasticity and aimed particularly on rationalization of the pronounced upturn in the experimental stress−strain curves of networks at higher elongation, including an interesting case of the bimodal networks.

S0024-9297(97)00069-7 CCC: $15.00
Published on Web 01/31/1998

Alternatively, using the procedure b, the force−length relation of single-chains can be evaluated[12−14] directly, without recourse to the distribution functions, by the simulation of the stretching "experiment" employing the MC method. The applied force may follow the chain vector or may act in the fixed direction (e.g., *z*-axis). This approach was extensively utilized in a series of papers by Kreitmeier et al.,[14−17] where the inhomogeneous deformation resulting in the globule−strand transition was described.

Both mentioned approaches, (a) and (b), and their modifications may also differ in constraints imposed on the chain ends. The usual assumption of the fixed end-to-end distance corresponds to the representation[2] of a chain as a spring of approximately zero unstrained length. Thus, in this type of constraint, the reference point of the vanishing force $f = 0$ is attained at $R = 0$ ("cyclic conformation") or in a close vicinity. However, in the treatment of coil swelling, a different type of constraint was employed.[18] One end of a coil is set to the origin and the other end is located anywhere in the spherical shell with radius R. The gradual swelling of a chain in a good solvent can be considered as an isotropic dilational stretching of a molecule. In this case the mean coil dimensions $\langle R^2\rangle^{1/2}$ in the dry unswollen state serve as the zero point of force. This reference state is closely related to the theory of elasticity of polymer networks where elongation is expressed relative to the dimensions in the undeformed state.

In our previous papers[13,19−21] we have investigated the single-chain relations force vs displacement by means of MC simulations of chains with EV using both described methodologies (a) and (b) combined with two different choices of the chain end constraints. For the $f-R$ relations calculated via non-Gaussian distribution function $W(R)$, the "spring deformation" constraints were assumed.[20,21] On the other hand the force vs displacement functions computed by procedure b and henceforth denoted as $F-R$, were based on the "coil deformation" constraints.[13] The stress-ensemble average was used in this case; i.e., the chain displacement R is calculated for a chain stretched with the preselected value of the load F. These simulations incorporated the intramolecular effects such as the chain flexibility and excluded volume due to the intrinsic volume of monomers (chain thickness) as well as due to the variable segment−segment interaction representing the solvent quality. Using the $F-R$ approach, the conformational transition globule−extended coil induced by the force F was found[13] in a bad solvent. Additionally, the computed internal force f was resolved[21] into the energy f_U and entropy f_S parts, which are related to the thermoelastic behavior of the networks.

In this paper it is our intention to address three aspects of the chain elasticity: (i) the variation of the force−displacement curves due to the solvent and type of constraints assumed, (ii) the elastic functions of a chain prestretched by an external force, and (iii) the mechanical response of (swollen) networks formed from these model chains.

At first we have compared the both types of relations, $f-R$ and $F-R$, computed by the MC technique for a single-chain in the Θ and athermal (good) solvents. The solvent-induced non-Gaussian behavior was found to be qualitatively similar for both types of elastic functions. However, the variation in the chain end constraints resulted in a marked change in the shape of the elastic functions for a given chain; i.e., the elastic response is altered due to the change of the physical situation.

Next, in analogy with the "unperturbed" distribution function $W(R)$ we have calculated the distribution function $W_F(R)$ corresponding to a coil prestretched by an external force F. The respective internal force f_F shows an enhancement of the stiffness of prestretched coils, the observation relevant to the finite extensibility of chains or possibly to the deformation of chains under shear flow.

Finally, the single-chain elastic functions were used to predict the mechanical response of a network using the three-chain affine junction model. Again, the variation of the stress−strain relations with the solvent quality was found in model networks. The relevance of the results of simulations to the so-called c* gels is discussed. The implications are analyzed of the solvent-induced non-Gaussian effects for the thermodynamics of swelling equilibrium in highly swollen gels.

Model and Method

The first step in the method used is universal for both approaches and involves generation and equilibration of chains. In the subsequent steps involving the chain deformation, the procedure differs in computations of forces f and F.

The chains of the length $N = 200$ segments with variable flexibility and intrachain contact energy (the solvent quality) were generated on a tetrahedral lattice. The conformational parameter ϵ_g, related by $e_g = \Delta\epsilon/kT$ to the gauche−trans energy difference $\Delta\epsilon$, was assumed zero for fully flexible chains. Some calculations were performed for $\epsilon_g = 1$, which corresponds approximately to the flexibility of a polymethylene (PM) chain. Conformations g^+g^+ and g^-g^- (the "pentane effect") were completely suppressed. In line with the previous papers[13,19−21] the chain thickness was accounted for explicitly by forbidding the occupation of the first neighbor sites on a lattice. Such a treatment of hard core repulsion of the distant segments represents the long-range analogy of the pentane effect (see Figure 1 in ref 19). The solvent effect was simulated by the reduced energy of intrachain segment−segment contacts $\epsilon_s = \epsilon_{ij}/kT$. Two regimes of the solvent quality ϵ_s were investigated: the athermal state ($\epsilon_s = 0$) and the Θ state, −0.58 for fully flexible chains and −0.55 for PM-like chains.[20]

The chain conformations were sampled by persistent reptation; the selection of the chain end that should move (and the rest of chain just follow) respected previous successful moves. The number of chain moves was in the range $(4-9) \times 10^7$. The distance R is expressed in units of a lattice spacing a; the mean-square end-to-end distance $\langle R^2\rangle$ was computed by a standard procedure.

From the equilibrium configurations of chains the force−displacement curves were determined by two methods. In the first, the traditional procedure of computation of the force f via the $W(R)$ function, the usual Metropolis algorithm, and the energy expression was employed. The radial distribution function of end-to-end distances

$$P(R) = 4\pi R^2\, W(R) \tag{3}$$

was obtained from the simulation by grouping similar chain vector lengths into a histogram with the interval

of one tetrahedral lattice spacing set to unity ($a = 1$). After conversion of $P(R)$ to $W(R)$, the free energy difference ΔA_{el} is calculated from eq 1. Subsequent differentiation for a chain with both ends constrained yields the force f acting in the direction of the chain vector ("spring deformation"). The statistical error of this procedure becomes intolerably high in the regions close to $R = 0$ and also at the high elongations of a chain. The number of gauche bonds p^g and the respective molar fraction x_g was evaluated for each interval span of the $W(R)$ distribution.

In the second method, the elastic response of single macromolecules computed via "experimental" procedure is described by the function F vs R. In this case one end of a coil is located in the origin and the other end is fixed on the surface of a sphere with radius R. By a stepwise increase of the external force F acting on both ends of a chain in the direction of instantaneous end-to-end vector **R**, the mean dimensions of the deformed coil were calculated for each particular F. In this "coil deformation" approach, the Boltzmann factor in the usual Metropolis sampling scheme reads as follows

$$w = \exp[-(E_{new} - E_{old})/kT]$$

$$(E_{new} - E_{old})/kT = \epsilon_s(n_{new} - n_{old}) + \epsilon_g(p^g{}_{new} - p^g{}_{old}) - (Fa/kT)(R_{new} - R_{old}) \quad (4)$$

where E is the total energy, n is the number of contacts each of reduced energy ϵ_s, p^g is the number of gauche bonds, and R is reduced by a. The subscripts describe microstates before and after the trial move. The external force F has no fixed orientation in space but follows the random moves of a chain and is always oriented in the direction of the chain vector.

Finally, as a partial combination of both above procedures, the function $W_F(R)$ is determined for a chain prestretched by an external force F, which obviously differs from the "unperturbed" distribution $W(R)$ in the absence of the force F. The function ΔA_F, defined with analogy with eq 1 for the distribution function $W_F(R)$ is computed, and subsequently, the related internal retractive force f_F of a macromolecule prestretched by an external force F is evaluated.

Results and Discussion

Force−Displacement Curves. At first we compare the force−displacement curves for the chains with 200 segments in athermal and Θ solvents. The curves were calculated (a) from the $W(R)$ distributions using the chain end constraints of the "spring deformation" type and (b) via an "experimental" approach using the "coil deformation" type of constraints (denoting forces in cases a and b by f and F, respectively). The difference between the type of constraints in cases a and b should be pointed out since the terms "spring" and "coil" are frequently used interchangeably in the polymer literature in discussion of chain elasticity. In plots of the elastic functions we use the relative displacement (the chain elongations) $r = R/\langle R^2\rangle^{1/2}$ and the reduced force $f\langle R^2\rangle^{1/2}/kT$, where $\langle R^2\rangle^{1/2}$ corresponds to the mean chain dimensions in a solvent assumed. In a similar vein, we define the reduced force $F\langle R^2\rangle^{1/2}/kT$; the mean dimensions in this case refer to the zero external force F, $\langle R^2\rangle_{F=0}{}^{1/2}$, but the subscript $F = 0$ will be omitted henceforth.

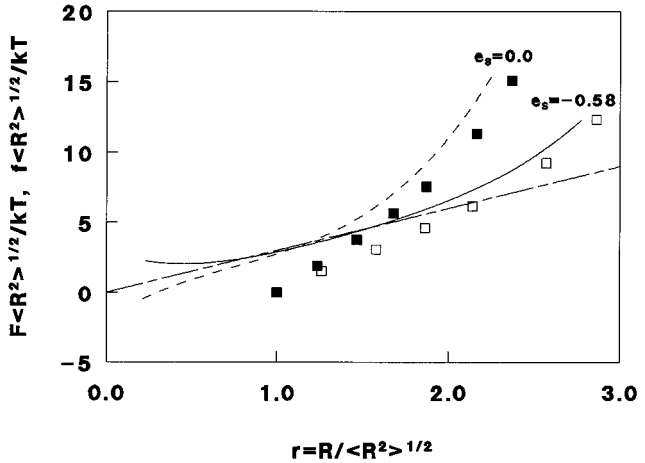

Figure 1. Force−displacement dependence in terms of reduced forces $f\langle R^2\rangle^{1/2}/kT$ (spring model) (curves) and $F\langle R^2\rangle^{1/2}/kT$ (coil model) (points) versus r for Θ (—, □) and athermal (- - -, ■) situations for fully flexible chains. The external force range is $Fa/kT = 0.0-0.4$ for both Θ and athermal chains. (- — -) depicts the Gaussian coil, eq 5.

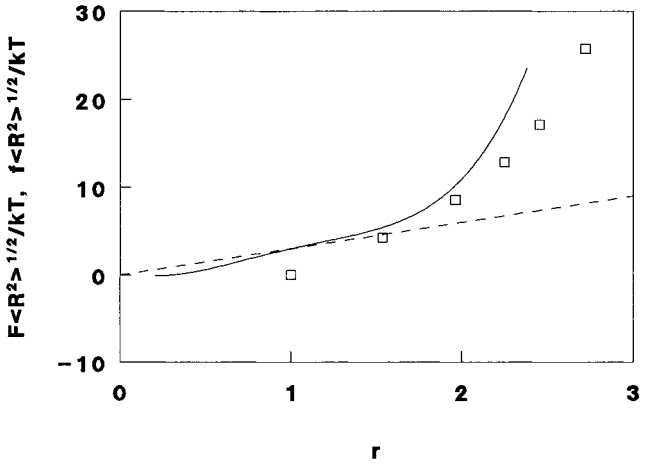

Figure 2. Force−displacement dependence in terms of reduced forces $f\langle R^2\rangle^{1/2}/kT$ (spring model) (—) and $F\langle R^2\rangle^{1/2}/kT$ (coil model) (□) versus r for athermal PM-like semiflexible chains, $\epsilon_g = 1.0$, $\epsilon_s = 0.0$, $Fa/kT = 0.0-0.6$. (- - -) depicts the Gaussian coil, eq 5.

The $f-r$ elastic functions of a fully flexible chain in two solvents are shown in Figure 1 and a similar plot for the PM-like chain in an athermal solvent is given in Figure 2. The linear function[2]

$$f_{id}\langle R^2\rangle^{1/2}/kT = 3r \quad (5)$$

which applies to the ideal Gaussian chains, is also given in Figures 1 and 2. The straight line crosses the origin in accordance with the concept of a Hookean entropy spring.

The elastic functions $f-r$ in Figures 1 and 2 calculated via the distribution $W(R)$ deviate from the linear dependence on r, particularly in the athermal solvent. The comparison of the elastic function for the athermal solvent to that for the Θ solvent makes possible a rough estimation of size of the EV effect and the effect of limited chain extensibility. The latter effect is presumably the sole source of the non-Gaussian behavior in the Θ solvent. It is established[2] that the limited chain extensibility becomes apparent from about one-third of the length of a fully stretched chain R_{max}. This rule-of-thumb is confirmed in our case of 200 segment chain,

where $R_{max} = 162.5$ and the corresponding maximum relative displacement r_{max} is 5.30 in the Θ chain. The deviations from linearity become actually apparent in Figure 1 at r about 1.7. Hence, we may assume that the additional steep upturn on the elastic curve of the athermal solvent at higher elongations with respect to the curve for the Θ solvent is due to the EV effect.

In contrast, in the region below $r = 1$ in the athermal solvent, the deviation from linearity is apparent at approaching $r = 0$, and close to $r = 0$ the force even becomes negative (compressive).[5] In all other regions of the elongation r in Figures 1 and 2 the force f is positive (tensile) for both solvents. The negative sign of force is a consequence of the drop in the non-Gaussian distribution function $W(R)$ in the region of cyclic conformations of the chain ("correlation hole"). The problem of the correlation hole is distinct in the plots of the functions $W(R)$ but is hidden in more frequently used plots of the $P(R)$ distributions.[7]

In addition to $f-r$ curves, derived Figures 1 and 2 show also the elastic functions $F-r$. The difference in the shape between these two sets of curves is immediately apparent and it is a consequence of the different constraints assumed for the chain ends (concerning the freedom in their fixation) in the spring deformation and coil deformation models. The concept of force f is based on the assumption[1,2] that both chain ends are fixed at the distance R in the direction of the chain vector. However, in the calculation of the force F, one end is fixed in the origin and the other end is located on the sphere with the radius R. An analogy can be noted in the case of models of the freely jointed chains: it was pointed out[4] that although the Kuhn−Grun and the Treloar results are equivalent for infinitely long chains with respect to the force−extension relation, the Treloar model describes a chain with fixed end-to-end distance (three constraints) whereas in the Kuhn−Grun results only the component of the end-to-end distance parallel to the extension is fixed (one constraint). Both computational procedures and the resulting f and F functions are related in a specific way, which resembles the interconnection between the probability density and radial chain vector distribution functions, $W(R)$ and $P(R)$, respectively.

Thus, the f and F elastic functions describe the different physical systems and the single-chain elastic response in Figures 1 and 2 differs in a similar way as differ the experimental stress−strain functions for a polymer material measured by the different deformation modes. Moreover, it is evident that the choice of the chain end constraints determines also the reference point of vanishing force on the elastic curve: in the spring model the zero-point $f = 0$ is attained at ring conformation $R = 0$ or in a close vicinity, whereas in the coil deformation model the zero-point force corresponds to the mean coil dimensions $\langle R^2\rangle^{1/2}$. As a consequence of the differing reference points, the force f is tensile in almost the whole range of r, whereas the force F is compressive at $r < 1$.

Qualitatively, the non-Gaussian effects in both sets of functions, $F-r$ and $f-r$, are similar. In the range of r between 1 and 2 the $F-r$ functions in Figure 1 were fitted by the following equation deduced in analogy with eq 5 for ideal chains

$$F\langle R^2\rangle^{1/2}/kT = \gamma(r - 1) \qquad (6)$$

The linear fit gives the slopes γ equal to 5.3 and 8.7 for the Θ and athermal systems, respectively. The slope γ increases with the improvement of the solvent quality and even in the Θ solvent γ is much higher than the value 3 assumed in ideal chains. Alternatively, the upturn in the $F-r$ elastic functions for athermal chains seen in Figures 1 and 2 can be described in the whole range of r by the scaling law $R \propto (Fa/kT)^x$. In our previous work[13] we found the value 0.61 for the scaling exponent x in flexible athermal chains.

As a note, we can mention that the coil deformation model and the ensuing zero-point force at $r = 1$ were introduced[18] in the theory of swelling of a flexible macromolecule. It is assumed that the swelling equilibrium is achieved at the point where an osmotic force is compensated by an elastic force due to the formation of the more extended conformations in a good solvent. Then the Helmholtz elastic energy of a coil is given by[18]

$$\Delta A_{coil} = kT[3/2(\alpha^2 - 1) - \ln \alpha^3] \qquad (7)$$

where the expansion coefficient of a coil $\alpha^2 = \langle R^2\rangle_{sw}/\langle R^2\rangle$ is defined by the ratio of the mean-square end-to-end distances of a swollen and a dry coil. This relationship should apply for the Gaussian chains if the uniform volume expansion of coils is assumed. By the subsequent differentiation according to α, the first term on the right-hand side of eq 7 yields the Hooke's force, eq 6, with $\gamma = 3$, provided that the expansion coefficient α is identified with the relative chain displacement r.

Summarily, it is pertinent in this part to point out that the single-chain force−displacement functions for macromolecules with the real chain features may strikingly differ from the universal Gaussian expression based on the "structureless" notion of a chain. The microstructural treatments, such as the Monte Carlo simulations, predict the more complex picture with the elastic functions depending on the chain lengths, the chemical structure, and conformation of the chains. Figures 1 and 2 document that the elastic response in chain deformation is also a sensitive function of the solvent quality. Moreover, our results demonstrate that the single-chain elastic function is affected by the particular details in the "deformation technique" (the chain-end constraints, the reference point of the vanishing force, etc.).

Chain Stretching and Conformational Equilibrium. The Helmholtz elastic energy of a chain determined by eq 1 can be resolved into the energy, ΔU, and entropy, $T\Delta S$, terms. The derivation of the energy term according to R yields the energy component of the force f_U and subsequently the ratio f_U/f. This ratio is used in the characterization of elastomers and can be determined from the thermoelastic (force−temperature) measurements. Recently, we have reported[21] the variation of f_U with R for some model chains in various solvents.

In the computational model used, the energetic factors may manifest themselves at deformation through the change of the contact energy on stretching or of the conformational energy, provided the conformers differing in energy are present in the chain. Either or both of these changes are inherent in the mechanism of elastic response as described by the curves in Figures 1 and 2. Hence, instead of the Gaussian (linear) entropic springs the nonlinear entropy-energy springs ought to be considered. The intersegmental contacts are broken, especially in the region of the compact confor-

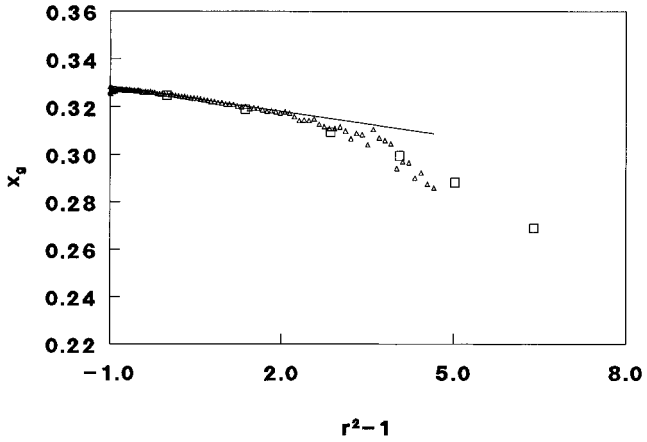

Figure 3. Fraction of gauche conformation x_g depending on stretching r for spring model with force f (△) and for coil model (□) with force F for PM-like semiflexible chains, $\epsilon_g = 1.0$, $\epsilon_s = 0.0$, $Fa/kT = 0.0-1.0$. The solid line represents the respective dependence given by eq 8.

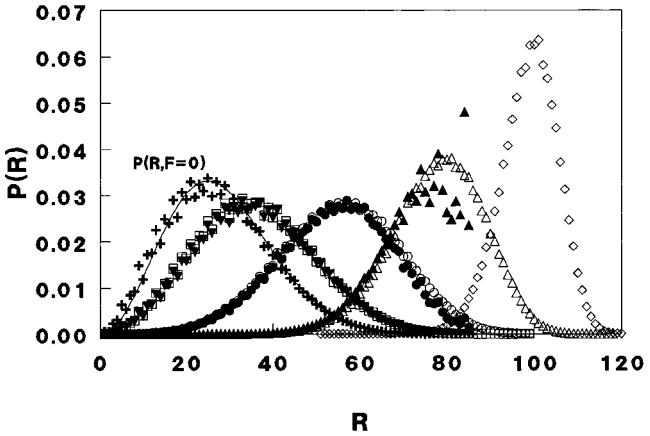

Figure 4. Distribution functions $P(R)$ of a fully flexible Θ ($\epsilon_g = 0$, $\epsilon_s = -0.58$) chain under variable external force $Fa/kT = 0.0$ (+), 0.05 (□), 0.15 (○), 0.3 (△), 0.6 (◇) from simulation. Respective distribution functions $P_F(R)$ constructed by eq 9 are plotted as (▼), (●), (▲). The full line curve depicts the Gaussian $P(R)$ function for given $\langle R^2 \rangle$ and $F = 0.0$.

mations at very small chain elongation r. In contrast, the gauche to trans isomerization on stretching is marked at high elongations r.

The rotational isomerization on stretching is illustrated in Figure 3 on the PM-like chain in the athermal solvent and the fraction of gauche conformation x_g is plotted here as a function of elongation r. The fraction x_g was determined by two different procedures consistent with the definitions of the force f and F. In the case of the force f, the fraction x_g is determined as an average from the chain configurations within the narrow interval of ΔR, whereas in the F procedure, x_g is determined as an ensemble average over all configurations available for a chain under the imposed force F.

It is seen from Figure 3 that both procedures predict the identical variation of x_g on r in the range of small and intermediate elongations. In other words, for a given R, the numbers of gauche bonds in a chain are identical, irrespective of how (by f or F) this R was realized. This finding contrasts with the difference between f and F procedures found in the force−displacement plots. At high elongations where the f concept is not applicable, the fraction x_g rapidly decreases, ultimately to the zero value in the limit of the fully extended zigzag form. In the range of small elongations, the dependence x_g vs r is well described by the function deduced[22] by using the rotation-isomeric theory of the coil stretching. This function, the decrease in the number of the gauche bonds with r, is expressed in our notation as

$$p^g = D_2 (r^2 - 1) \tag{8}$$

where for PM chains[22] the coefficient $D_2 = -0.656$. However, as is seen in Figure 3, the relation (8) increasingly underestimates the extent of the isomerization at r above about 1.3. Thus, for example, by the chain elongation from $r = 1$ to $r = 2$ the relative population of gauche bonds x_g is reduced by about 0.015 according to the MC data in Figure 3 but eq 8 predicts in this interval the decrease of x_g by about 0.01 only.

Distribution Function $W_F(R)$ in External Fields. One can consider also the procedure where the both concepts, of internal force f and of external force F, are combined as in the investigation of the elastic response of a macromolecule prestretched by an external force F. Subsequently, the distribution function and the corresponding force, denoted as $W_F(R)$ and f_F, respectively, can be evaluated for this prestretched chain. It is assumed[6,23] that the resulting probability density distribution function $W_F(R)$ is proportional to the function $W(R)$ of an undeformed macromolecule (when $F = 0$) corrected by the factor $\exp(FR/kT)$

$$W_F(R) = \kappa(F)\, W(R) \exp(FR/kT) \tag{9}$$

The normalization coefficient $\kappa(F)$ is a function of the applied force F. The related radial distribution function $P_F(R)$ can be defined by the substitution of eq 3 into eq 9.

We have tested the applicability of the transformation of the distribution functions $P(R)$ into $P_F(R)$ by the exponential relationship, eq 9, for the fully flexible chain in the Θ solvent and for three values of the reduced external force Fa/kT (Figure 4). The distribution functions $P_F(R)$ from MC simulations were compared with the analogous functions $P_F(R)$ resulting from eq 9 using the normalization factor $\kappa(F)$ optimized to secure the best fit of these two functions. At small and moderate external forces F the coincidence is very good. At high values of F the comparison is precluded due to almost negligible population of states in the distribution function $W(R)$ at these values of extension r. In general, the external force F modifies the shape of the $W(R)$ function in a manner similar to the large EV effect: the external force F enlarges the inaccessible region around $R = 0$, i.e., increases the correlation hole.

The distribution functions $W_F(R)$ can be transformed using eq 1 into the related plots of ΔA_F vs R. This transformation, including the value ΔA_{el} for the undeformed chain ($F = 0$), is shown in Figure 5 for the fully flexible chain in the Θ solvent. The external force F gradually shifts the minimum on the curves in Figure 5 further away from quasi-cyclic structures of the chains and destabilizes the conformations of the chains on the left side of the minimum. In the terminology of the non-Hookean spring model, the mixed entropy-energy tendency for the spring contraction is counterbalanced in the minimum R_m by the chain prestretching due to the external force F.

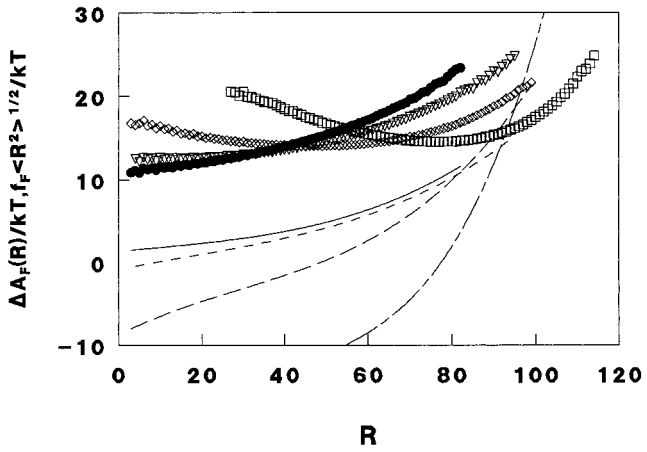

Figure 5. Free energy changes ΔA_F (●, ▽, ◇, □) and respective reduced elastic forces (full line, dash, long dash, dash dot) of a fully flexible Θ ($\epsilon_g = 0$, $\epsilon_s = -0.58$) chain under variable external force $Fa/kT = 0.0, 0.05, 0.15, 0.3$.

The balance of the two above factors also determines the sign of the force in the elastic functions f_F vs R deemed to be appropriate for the description of elastic response of coils prestrained by the external force F (Figure 5). In this case the mean dimensions $\langle R^2\rangle_F^{1/2}$ for the prestrained chain were used in calculations of the product $f_F\langle R^2\rangle_F^{1/2}/kT$. By an increase of the prestretching force F the elastic curves become steeper, in correspondence with the notion that chains are already fairly extended in the prestretched state and their additional elongation requires a considerable load. The negative force f_F is present in the region of the chain compression at $R < R_m$.

The analysis of the elastic response of the model flexible chains prestretched by the external force F may be directly relevant to the macromolecules deformed in a hydrodynamic field and to the finite extensibility of chains. The enhanced steepness of the curves f_F vs R in Figure 5 indicates that the hydrodynamic field can increase the effective stiffness of coils. Hence, the sole replacement of the Gaussian theory by the non-Gaussian approach, but still disregarding the force F, might not be a sufficient improvement and the prestretching of coils should be accounted for in the description of their elastic behavior in the hydrodynamic field. These findings are corroborated by a recent report of a transition from the coiled to stretched state by a hydrodynamic field,[24] which was found sharper in poor solvents than in good solvents. In our Figure 1 we observe similarly the higher sensitivity of the Θ chain toward deformation by external force F in comparison to the athermal chain.

In analogy with the functions related to the external force F, the distribution function appropriate for any external field $W_\xi(R)$ and the corresponding relations ΔA_ξ vs R and f_ξ vs R can be defined. The confined systems represent a relevant example, and the constraints on chains due to the walls of the cylinder, tube, slit, etc., or due to the surrounding molecules as in liquid crystals, may affect the plots ΔA_ξ vs R and f_ξ vs R in a similar way as the excluded volume or the uniaxial force: the enhanced constraints produce the large correlation hole in the function $W_\xi(R)$ with the consequent impacts on all derived functions. This reasoning is supported by the observation that the function ΔA_ξ vs R obtained from MC simulations for a chain confined by two impenetrable walls[25] displays a minimum shifted to the right side relative to the unconfined situation, in full correspondence with the behavior of curves in Figure 5.

Non-Gaussian Behavior of Swollen Networks. The non-Gaussian single-chain relations for flexible macromolecules of the type $f-r$ can be utilized in the prediction of the elastic equation-of-state for the swollen polymer networks using the standard "three-chain model".[2,4,8−11] In the three-chain model all chains in a network are replaced by three effective chains with the end-to-end distances R_i ($i = x, y, z$) parallel to the coordinate axes. The deformation in the affine limit at constant volume is assumed, where the cross-links move linearly with the macroscopical dimensions of the sample L_i. The respective macroscopic deformations of a sample are defined as elongations $\lambda_i = L_i/L_{i0}$ where subscript zero denotes the undeformed dimensions. In the case of uniaxial elongation in the direction of the x-axis this simplifies to $\lambda_x = \lambda$ and $\lambda_z = \lambda_y = \lambda^{-1/2}$. Then, the total elastic Helmholtz energy ΔA_{net} for a network composed of the ν chains per volume unit is given by the difference of the Helmholtz energy in the deformed and undeformed state[2]

$$\Delta A_{net} = (\nu kT/3)\,[A_{el}(R_0\lambda) + 2A_{el}(R_0\lambda^{-1/2}) - 3A_{el}(R_0)] \quad (10)$$

where A_{el} is the single-chain Helmholtz energy from eq 1 and R_0 is the average chain dimension of the network chains in the undeformed state.

The derivation of the above relation with respect to elongation at constant volume and temperature yields the equilibrium elastic force per unit undeformed cross-sectional area A^* (nominal stress $f^* = f/A^*$)[2,10,11]

$$f^* = \nu kTR_0/3[f_1(R_0\lambda) - \lambda^{-3/2}f_1(R_0\lambda^{-1/2})] \quad (11)$$

Thus in the three-chain model the overall force for a network can be expressed[4] by means of the single-chain elastic functions $f_1(R)$. The product νkT in the front factor of the above equation can be replaced by $\rho RT/M_c$, where ρ is the network density and M_c is the average molecular weight of a chain between cross-links.

The three-chain model is a rather crude approximation of a network and its improvements were suggested such as the tetrahedron (four-chains) model[2] and the eight-chain model.[26] The increased number of chains in a network model oriented in various directions should improve the averaging out of the contribution to the Helmholtz energy over all chain orientations. The general treatments of the orientation distribution of molecular chains have been formulated,[2,27] which are applicable for rubber networks but require numerical integration. However, all these modifications of the three-chain model do not remove the other more fundamental limitations in the present network theory[3] such as postulations on the affine deformation and on the fluctuations in junction points, the neglecting of slip-links and other network defects, and particularly, the independence of interchain interaction in network on deformation.

The three-chain model combined with non-Gaussian distributions $W(R)$ and various modifications of eq 11 were already used[8−11] in the rationalization of the experimental stress−strain curves of the dry networks. As a starting point, the $W(R)$ functions derived[8,9] using the high even moments $\langle R^{2x}\rangle$ were employed, or in the

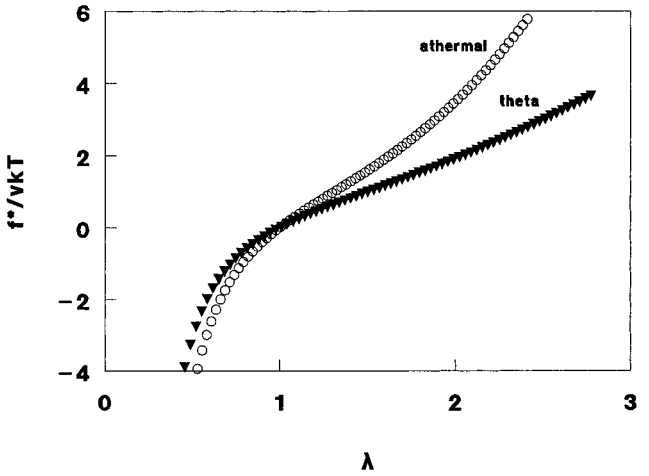

Figure 6. Nominal stress $f^*/\nu kT$ versus extension λ for Θ (▼) and athermal (○) fully flexible chains in a model network.

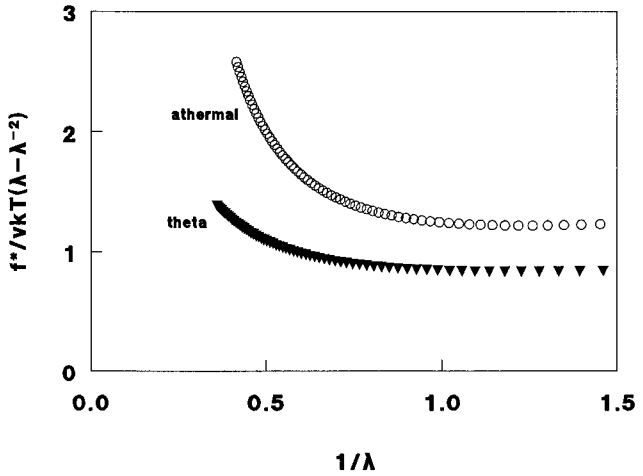

Figure 7. Mooney−Rivlin plot for Θ (▼) and athermal (○) fully flexible chains in a model network.

related studies[10,11] the realistic rotational isomeric state model combined with MC sampling was adopted for the calculation of $W(R)$ functions for several types of chains of various complexity. The non-Gaussian distribution functions were then used to calculate the stress−strain isotherms of the dry polymer networks including the interesting case of the bimodal networks.[8−11] In a modified approach[28] the elastic force was calculated from the total deformation of the chain vectors in a random array of chains, rather than from the deformation of an "average" chain.

In contrast to dry networks, the intra- and interchain excluded volume effects cannot be neglected in swollen networks. The application of our single-chain simulation data to the prediction of the mechanical response of swollen networks by the three-chain model is particularly well justified[29] for the gels prepared by cross-linking at concentrations close to c^* (the threshold overlap concentration of semidiluted chains). In these gels, denoted as c^* gels, the network strands should behave as isolated chains. In the blob picture each strand of the network forms a blob of the size of an isolated chain. The blobs are closely packed, but the strand displays single-chain behavior inside one blob. The intrachain entropy changes and the energy changes due to the conformational isomerization and variations in number of contacts, summed throughout individual chains furnish the corresponding quantities for a network, in accordance with the assumptions in the traditional theory of rubber-like elasticity.

Using eq 11 we have transformed the single-chain $f-r$ functions from Figure 1 for fully flexible chains in the Θ and athermal solvents to the stress−strain isotherms of the swollen networks (Figure 6). The overall shape of the curves in Figures 1 and 6 is similar, and their sensitivity to the quality of solvent is not affected by the transformation. The only marked difference between functions in Figure 1 and in Figure 6 is connected with the change of the reference point of vanishing force, from $r = 0$ to $r = \lambda = 1$, which accompanies the transfomation. In other words, the conversion of the single-chain forces $f_1(R)$ to the nominal stress f^* for a network according to eq 11 is accompanied by the replacement of the spring deformation model by the coil deformation model. Consequently, a broad region of the network compression ($\lambda < 1$) is seen in Figure 6, which is absent in the single-chain plots in Figure 1.

The functions in Figure 6 were further recast using the semiempirical Mooney−Rivlin relationship[2,3] (Figure 7)

$$f^*/\nu kT\,(\lambda - \lambda^{-2}) = 2C_1 + 2C_2\lambda^{-1} \qquad (12)$$

This representation is preferred in the comparison of theory with experimental data. The horizontal line in this plot would indicate the Gaussian behavior. The non-Gaussian features, excluded volume, and limited chain extensibility are responsible for upturns in the reduced stress in Figure 7. Similarly as in single-chain curves, we again assume that limited chain extensibility is the only factor contributing to the upturn, or positive $2C_2$ correction, in the Θ solvent. The enhanced steepness of the elastic curve in the athermal solvent at small values of λ^{-1} with respect to the curve for the Θ solvent is due to the EV effect.

The results in Figures 6 and 7 are directly relevant to c^* gels but indirectly also to the other swollen networks. The striking solvent effect on the elastic response of a network originated in our simulations from the intrachain EV effect should be significant in highly swollen gels and its role would diminish by the reduction of the degree of swelling.

The finding of the solvent-sensitive elastic functions of chains constituting a network suggests a modification of the thermodynamic treatment of swelling of networks. The theory assumes[3] that the change of Helmholtz energy ΔA_{sw} is composed of two terms: the change in the Helmholtz energy of mixing ΔA_{mix} and change in the Helmholtz elastic energy of the network ΔA_{net} upon the isotropic dilatation with the introduction of a solvent. The first term is usually represented by the Flory−Huggins relationship and is independent of the elongation of a network. The solvent quality is accounted for in this term through the interaction parameter χ. The second, elastic, term is usually approximated by the affine network model of the Gaussian chains and thus assumed independent of the type of solvent used. The solvent-sensitive $f-r$ relations predicted by our simulations suggest that the mixing and elastic terms in the Helmholtz energy of swelling are not fully separable, at very least not in the highly swollen gels. The elastic term may thus depend on the solvent quality and on the polymer concentration.

Conclusions

We have found that the single-chain force-elongation functions $f-r$ and $F-r$ computed by the MC technique are strikingly affected by the chain-end constraints chosen, either of the "spring deformation" type in which zero-point force corresponds to the cyclic conformation of the chain or of the "coil deformation" type in which the vanishing force is associated with the mean coil dimensions. Even though the terms spring and coil are frequently used interchangeably in the polymer literature, the inherent models correspond to different physical situations and the specification of the type of constraints is imperative for the analysis of chain elasticity.

The computed single-chain elastic functions show the non-Gaussian behavior at moderate and high elongations as a result of the limited chain extensibility and in athermal solvent additionally due to the intrachain (solvent) excluded volume effect. This solvent dependence was found to be qualitatively similar for both types of elastic functions.

In a flexible macromolecule prestretched by an external force F, the appropriate distribution function $W_F(R)$ was calculated and the validity of its relation to the "unperturbed" function $W(R)$ via eq 9 was verified. The plots of the respective internal force f_F reflect an enhancement of the stiffness of prestretched coils.

Finally, the single-chain elastic functions were employed in the prediction of the mechanical response of a (swollen) network using the three-chain affine model. In the model networks, again, the variation of the stress−strain isotherms with the solvent quality was observed. The direct relevance of the simulation results to the mechanical properties of the so-called c^* gels (where the interchain EV effect can be neglected) was emphasized. The implications are analyzed of the solvent-sensitive elastic functions of network chains for the separability of the mixing and elastic terms in the Helmholtz energy of swelling of networks.

Acknowledgment. The authors are grateful to the Grant Agency for Science (GAV), grant No. 2/4019/97 for partial support of this work.

References and Notes

(1) Flory, P. J. *Statistical Mechanics of Chain Molecules*; Wiley-Interscience: New York, 1969.
(2) Treloar, L. R. G. *The Physics of Rubber Elasticity*; Claredon Press: Oxford, U.K., 1975.
(3) Mark, J. E.; Erman, B. *Rubberlike elasticity, a molecular primer*; J. Wiley: New York, 1988.
(4) Glatting, G.; Winkler, R. G.; Reineker, R. *Macromolecules* **1993**, *26*, 6085.
(5) Gao, J.; Weiner, J. H. *Macromolecules* **1987**, *20*, 142.
(6) Oono, Y.; Ohta, T.; Freed, K. F. *Macromolecules* **1981**, *14*, 880.
(7) Bishop, M.; Clarke, J. H. R.; Rey, A.; Freire, J. J. *J. Chem. Phys.* **1991**, *95*, 4589.
(8) Llorente, M. A.; Rubio, A. M.; Freire, J. J. *Macromolecules* **1984**, *17*, 2307.
(9) Menduina, C.; Freire, J. J.; Llorente, M. A.; Vilgis, T. *Macromolecules* **1986**, *19*, 1212.
(10) Mark, J. E.; Curro, J. G. *J. Chem. Phys.* **1983**, *79*, 5705.
(11) Erman, B.; Mark, J. E. *J. Chem. Phys.* **1988**, *89*, 3314.
(12) Okamoto, H.; Ohde, Y. *J. Chem. Phys.* **1986**, *84*, 7048.
(13) Cifra, P.; Bleha, T. *Macromol. Theory Simul.* **1995**, *4*, 233.
(14) Wittkop, M.; Sommer, J.-U.; Kreitmeier, S.; Goritz, D. *Phys. Rev. E* **1994**, *49*, 5472.
(15) Kreitmeier, S.; Wittkop, M.; Goritz, D. *J. Comput. Phys.* **1994**, *112*, 267.
(16) Wittkop, M.; Kreitmeier, S.; Goritz, D. *Comput. Polym. Sci.* **1995**, *5*, 187.
(17) Wittkop, M.; Kreitmeier, S.; Goritz, D. *J. Chem. Soc. Faraday Trans.* **1996**, *92*, 1375.
(18) Flory, P. J. *J. Chem. Phys.* **1949**, *17*, 303.
(19) Cifra, P.; Bleha, T. *Polymer* **1993**, *34*, 3716.
(20) Cifra, P.; Bleha, T. *Makromol. Theory Simul.* **1995**, *4*, 40.
(21) Cifra, P.; Bleha, T. *J. Chem. Soc., Faraday Trans.* **1995**, *91*, 2465.
(22) Abe, Y.; Flory, P. J. *J. Chem. Phys.* **1970**, *52*, 2814.
(23) Curro, J. G.; Schweizer, K. S.; Adolf, D.; Mark, J. E. *Macromolecules* **1986**, *19*, 1739.
(24) Haligoglu, T.; Bahar, I.; Erman, B. *J. Chem. Phys.* **1996**, *105*, 2919.
(25) Varyukhin, S. E.; Zaitsev, M. G. *Polymer* **1990**, *31*, 1750.
(26) Arruda, E. M.; Boyce, M. C. *J. Mech. Phys. Solids* **1993**, *41*, 389.
(27) Wu, P. D.; van der Giessen, E. *J. Mech. Phys. Solids* **1993**, *42*, 427.
(28) Stepto, R. F. T.; Taylor, D. J. R. *J. Chem. Soc., Faraday Trans.* **1995**, *91*, 2639.
(29) Everaers, R. *J. Phys. II (France)* **1995**, *5*, 1491.

MA9700690